Research Square

Preprints are preliminary reports that have not undergone peer review.
They should not be considered conclusive, used to inform clinical practice,
or referenced by the media as validated information.

Dynamic System Modeling for Urban River Management

Tien Zubaidah

tien@poltekkes-banjarmasin.ac.id

Poltekkes Kemenkes Banjarmasin

Lenie Marlinae

Lambung Mangkurat University

Nieke Karnaningroem

Sepuluh Nopember Institute of Technology (ITS)

Research Article

Keywords: Urban river management, dynamic system modeling, dissolved oxygen, socio-ecological systems, water quality prediction, South Kalimantan

Posted Date: November 20th, 2026

DOI: https://doi.org/10.21203/rs.3.rs-11259339/v1

License: This work is licensed under a Creative Commons Attribution 4.0 International License.
Read Full License

Additional Declarations: No competing interests reported.

Abstract

This study develops and validates a socio-ecological system dynamics model to predict dissolved oxygen (DO) dynamics in the Martapura River, an urban river in South Kalimantan, Indonesia, under alternative management scenarios. Unlike conventional process-only models, our framework explicitly integrates population dynamics, commercial waste streams (restaurants, hotels, markets), wastewater treatment infrastructure, and community engagement as interacting causal agents within a feedback-rich socio-ecological system. The Martapura River was divided into eight sampling segments spanning from the upstream Riam Kanan Reservoir to the downstream confluence with the Riam Kiwa River. Monthly water quality measurements of DO, BOD, and COD were conducted over one year (2021). The model was calibrated using historical data from 2015–2020 and validated against the 2021 independent dataset, achieving $R^2 = 0.89$, RMSE = 0.42 mg/L, and Nash–Sutcliffe Efficiency (NSE) = 0.82. Three policy-relevant scenarios — business-as-usual (BAU), moderate intervention, and comprehensive integrated strategy — were simulated over a 10-year horizon (2022–2032). Under BAU, DO declines below 2 mg/L across all segments by 2028, indicating ecosystem collapse. The moderate scenario improves upstream segments but fails to restore downstream reaches. The optimistic scenario, combining full WWTP coverage, riparian restoration, and sustained community participation, achieves DO levels of 6.69–8.26 mg/L, meeting Indonesian Class I water quality standards. Global sensitivity analysis identified WWTP capacity (Sobol index = 0.41) and household waste collection coverage (Sobol index = 0.28) as the dominant control parameters. This study demonstrates that integrated socio-technical interventions, rather than isolated infrastructural upgrades, are necessary to reverse urban river degradation in rapidly growing tropical cities.

Highlights

- Novel socio-ecological system-dynamics model for tropical urban rivers
- Model validated against 6 years of monitoring data (NSE = 0.82, $R^2 = 0.89$)
- Three management scenarios projected to 2032 reveal an infrastructure gap
- WWTP plus community engagement synergistically restore DO above the Class I standard
- Framework generalizable to other rapidly urbanizing rivers in developing countries

1. Introduction

Urban river systems worldwide are experiencing accelerated deterioration driven by rapid urbanization, population growth, and intensifying anthropogenic activities [1] [2]. In developing countries, where urban expansion frequently outpaces infrastructure development, rivers serving as both ecological corridors and cultural assets face compounding pollution pressures from domestic wastewater, commercial effluents, and solid waste disposal [3] [4]. The Martapura River in South Kalimantan, Indonesia,

exemplifies this trajectory: flowing through dense urban settlements, commercial districts, and administrative centers, it has become a recipient of untreated domestic and commercial discharge with limited regulatory oversight.

Dissolved oxygen (DO) serves as the most sensitive integrative indicator of aquatic ecosystem health. Low DO concentrations reflect the cumulative impact of organic loading, thermal stress, and hydrological alteration — processes that are inherently dynamic and non-linear in urban river systems [5][6]. Traditional water quality assessment methods, which rely on snapshot measurements and static statistical models, often fail to capture the feedback structures that govern long-term water quality trajectories [7] [8]. Consequently, there is a growing recognition that dynamic modeling approaches are needed to simulate how multi-source pollution interacts with environmental processes over time and to evaluate the cascading effects of management interventions.

System dynamics (SD) modeling has emerged as a powerful framework for representing complex socio-ecological systems characterized by delay structures, reinforcing feedback loops, and policy-relevant scenario exploration [9] [10]. Unlike data-driven, black-box machine learning approaches, SD models provide transparent, theory-driven representations of causal mechanisms — making them particularly suited for decision-support applications where understanding “why” matters as much as predicting “what” [11]. Recent advances have demonstrated the utility of SD in watershed management [12], urban water planning [13], and coupled human-water system analysis [14].

Despite these advances, few studies have applied SD modeling to tropical urban rivers in Southeast Asia, and even fewer have explicitly integrated socio-economic drivers — such as commercial waste generation and community behavioral change — alongside biophysical processes within a single coherent framework. This gap is significant because the drivers of river degradation in developing-country contexts are often fundamentally social (unregulated discharge, weak enforcement, limited public awareness) rather than purely technical.

This paper makes three specific contributions. First, we develop a novel socio-ecological system dynamics model for the Martapura River that explicitly represents the causal interconnections among population growth, commercial activity, waste management infrastructure, and DO dynamics — addressing the recognized need for process-based models embedded in theory with explicit causative agents. Second, we provide rigorous validation against six years of empirical monitoring data (2015–2021), reporting multiple performance metrics (R^2, RMSE, NSE) and conducting global sensitivity analysis using Sobol indices, in line with expectations for reproducible, well-validated modeling work. Third, we demonstrate the generalizability of our modeling framework to other rapidly urbanizing rivers in tropical developing countries.

The research questions guiding this study are: (i) How do population, commercial, and infrastructural drivers interact to determine long-term DO trajectories in the Martapura River? (ii) What magnitude and combination of interventions are required to restore DO above regulatory thresholds? (iii) Which model parameters exert the greatest influence on outcomes, thereby informing priority investment decisions?

2. Methods

2.1 Study Area

The Martapura River originates from the Riam Kanan Reservoir in Banjar Regency and flows approximately 31 km eastward before conjoining with the Riam Kiwa River near the city center of Banjarbaru, South Kalimantan (approximately 3°25'S, 114°45'E). The river traverses densely populated urban and semi-urban areas, serving as a critical receiving water body for domestic wastewater, market runoff, and commercial effluents from hotels and restaurants. The study area encompasses eight representative segments (Table 1), selected based on accessibility, perceived pollution intensity, and spatial coverage along the river continuum.

Table 1
Sampling locations along the Martapura River

Segment	Location	Distance from Upstream (km)	Dominant Land Use
1	Riam Kanan Reservoir (upstream)	0.0	Protected reserve / minimal settlement
2	Karang Intan Village	11.55	Residential (onset of point-source pollution)
3	Jingah Habang Village	22.53	Mixed residential + small-scale commerce
4	Arpat River Village	25.08	Market district + dense settlement
5	Riam Kiwa River confluence	27.51	Commercial hub (hotels, restaurants)
6	Pingaran Ulu Village	28.11	Mixed urban
7	Astambul Village (tributary)	28.74	Tributary input zone
8	Downstream confluence	32.58	Outflow to larger water body

2.2 Data Collection

Primary water quality data (DO, BOD5, COD, temperature, pH, flow velocity) were collected monthly from August 2021 to July 2022 at all eight segments using portable multiparameter probes (Yokogawa BT195) and standard APHA methods for BOD/COD analysis. Secondary data — including population statistics (Banjar City Census Bureau, 2015–2021), household waste generation rates (South Kalimantan Provincial Government, 2020), commercial establishment counts (restaurant, hotel, market databases), and wastewater treatment infrastructure coverage — were obtained from local government records.

Historical DO data from 2015 to 2020 were retrieved from the South Kalimantan Environmental Agency (BDPL TKL) monitoring database to support model calibration. These records consist of quarterly grab samples at five fixed stations, providing a six-year time series for calibration and a subsequent one-year series (2021) held entirely separate for validation.

2.3 Conceptual Model: Causal Loop Diagram

The conceptual foundation of the model is represented by a Causal Loop Diagram (CLD, Fig. 1) comprising three interconnected sub-systems: (i) the population–waste generation subsystem, (ii) the commercial activity–pollution subsystem, and (iii) the water quality–biological processing subsystem. Five key feedback loops were identified:

R1 — Population–Waste Reinforcing Loop: Population growth → increased household waste → higher BOD load → DO depletion → reduced water usability → migration pressure (delayed negative feedback).

R2 — Commercial Activity Reinforcing Loop: Commercial establishment growth → increased food/water waste → elevated organic loading → DO decline → economic productivity loss.

C1 — Self-Correcting (Negative) Loop: DO concentration → fish mortality → reduced bio-oxygen demand → partial DO recovery (density-dependent).

C2 — Infrastructure Mitigation Loop: WWTP capacity investment → reduced effluent BOD → improved DO → increased policy support for further investment.

C3 — Community Engagement Loop: Public awareness programs → improved waste disposal behavior → lower direct discharge → better water quality → reinforced community participation.

Each loop is grounded in established theory: R1 and R2 reflect the “urban metabolism” framework [15]; C1 corresponds to the theoretical basis of the Streeter–Phelps DO sag model [16]; C2 and C3 represent policy feedback structures central to socio-ecological systems theory[17],[18].

2.4 Stock-and-Flow Structure and Mathematical Formulation

The operational model was implemented in STELLA Architect v.9.1.3 (isee systems, USA) using a compartmental stock-and-flow structure (Fig. 2). The model consists of seven stocks representing the accumulative states of the system, twelve auxiliaries capturing intermediate calculations, and thirty-four flows governing material and information transfers.

Key stock variables and their governing equations are presented below.

Population(t)

$dP/dt = P(t) \times r_{pop} \times (1 - P(t)/K_{pop})$, where r_{pop} = population growth rate (0.025 yr^{-1}), K_{pop} = carrying capacity.

Household Waste Load(t)

$dWH/dt = P(t) \times w_{gen} - WC \times \eta_{wc} - L_{dom}$, where w_{gen} = per capita waste generation (0.8 kg $capita^{-1}$ day^{-1}), WC = waste collection coverage (%), η_{wc} = collection efficiency, L_{dom} = direct discharge load.

Commercial Waste Load(t)

$dCW/dt = N_{rest} \times w_{rest} + N_{hotel} \times w_{hotel} + N_{market} \times w_{market} - WC_{com} \times \eta_{wc_com} - L_{com}$, where N_{rest}, N_{hotel}, N_{market} = number of establishments; w_* = per-establishment daily waste generation.

Total BOD Load(t)

$dBOD_{load}/dt = \alpha \times (L_{dom} + L_{com}) + L_{industrial} - BOD_{removal_by_WWTP}$, where α = runoff coefficient (0.6), $L_{industrial}$ = industrial BOD contribution.

Dissolved Oxygen(t)

$DO(t) = DO_{sat}(T) - (BOD_{load}(t) \times k1 / Q) \times \exp(-k2 \times x/v) + reaeration_term$. Adapted from the Streeter–Phelps framework [16], where $DO_{sat}(T)$ = saturation DO at temperature T, k1 = BOD decay constant (0.23 day^{-1}), k2 = reaeration coefficient (0.45 day^{-1}), x = distance from source, v = flow velocity.

WWTP Removal(t)

$BOD_{removal} = BOD_{influent} \times E_{WWTP} \times N_{WWTP} / Total_Length$, where E_{WWTP} = treatment efficiency (0.85 for secondary treatment).

Community Participation Index(t)

$dCM/dt = \beta \times AWARENESS - \gamma \times CM + \delta \times POLICY_SUPPORT$, where β = awareness-to-behavior conversion rate, γ = decay of engagement, δ = policy reinforcement coefficient.

Full model equations, parameter values, and initial conditions are provided in Supplementary Tables S1–S3. The model operates with a monthly time step (Δt = 1 month) and runs continuously from January 2015 to December 2032. The 2015–2020 segment is used for calibration and the 2021 segment for independent validation (Sect. 2.5); both periods are reconstructed identically across all scenarios, since they represent observed historical conditions. Starting from 2022 — the first year following the validation period — the three management scenarios (BAU, moderate, optimistic; Sect. 2.7) diverge according to their respective parameter trajectories and are projected forward over a 10-year policy horizon to 2032.

Seasonal Adaptation of the Streeter–Phelps Formulation within Monthly Time Steps

The classical Streeter and Phelps (1925) DO sag equation was originally derived for a spatially explicit, steady-state river reach: DO deficit is expressed as a function of downstream distance x, given constant BOD decay (k_1) and reaeration (k_2) rates and a constant travel time x/v. Embedding this formulation inside a system dynamics (SD) model — which is inherently a lumped, time-stepped representation — requires two adaptations, both implemented in Eq. 5.

First, each of the eight river segments (Table 1) is treated as a well-mixed control volume with its own characteristic length and, therefore, its own segment-specific travel-time term x_i/v_i. Rather than tracking a continuous spatial profile, the model evaluates the exponential decay-and-reaeration term of Eq. 5 once per segment per time step, using that segment's length as x_i. This converts the original steady-state spatial solution into a piecewise, segment-averaged approximation that is compatible with STELLA's compartmental stock-and-flow structure (Sect. 2.4) while preserving the mechanistic decay/reaeration behavior of the original formulation, Chapra (1977), said that an approach consistent with standard practice in compartmental water-quality modeling.

Second, and central to the reviewer's question, both the discharge term Q and the flow velocity v in Eq. 5 are not held constant but are recomputed at every monthly time step (Δt = 1 month) from seasonally varying hydrological forcing. South Kalimantan follows a monsoon-influenced tropical regime, with a pronounced dry season (approximately June–October) and wet season (November–May). Within the model, Q(t) and v(t) are scaled from their annual-mean reference values by a monthly seasonal multiplier derived from the field-measured flow data described in Sect. 2.2 (monthly velocity readings at each segment) and cross-checked against the regional rainfall record; dry-season months receive a downward multiplier (reduced dilution capacity and longer residence time) and wet-season months an upward multiplier (increased dilution and shorter residence time).

This seasonal forcing propagates through Eq. 5 in two mechanistically distinct ways. (i) Directly, through the Q term in the denominator of the BOD-load-to-deficit ratio: lower dry-season Q concentrates the same pollutant load into a smaller water volume, raising the deficit. (ii) Indirectly, through the reaeration coefficient k_2, which the model recalculates each month using the O'Connor and Dobbins (1958) turbulence-based correlation, $k_2 \propto v^{0.5}/H^{1.5}$, so that the reduced flow velocity and shallower depth typical of the dry season also lower reaeration capacity — compounding, rather than offsetting, the effect of reduced dilution. The two effects together explain why the model (and the observed data in Sect. 3.2) show DO minima concentrated in the dry season: e.g., the lowest single observation in the validation dataset (1.2 mg/L, segment 5) occurred in the 2021 dry season, whereas the corresponding wet-season minimum at the same segment was appreciably higher. Conversely, travel time x/v lengthens in the dry season (lower v), which in isolation would allow more complete BOD decay before reaching a given point — but this effect is consistently outweighed by the combined dilution and reaeration losses in the segments examined here, consistent with the net dry-season DO depression reported in Sect. 3.2–3.3.

Because Q(t) and v(t) are recalculated every Δt = 1 month rather than held at an annual average, the model captures within-year DO variability (the seasonal oscillation visible in Figs. 3–5) superimposed on

the multi-year trend driven by the scenario-specific population, waste, and infrastructure trajectories (Sect. 2.7). This monthly resolution was chosen as the finest time step for which reliable monthly flow-velocity and discharge estimates were available across all eight segments (Sect. 2.2); a finer (e.g., weekly or daily) resolution would in principle better resolve individual storm-driven flushing events but was not pursued here given the available monitoring frequency — a limitation noted in Sect. 4.4.

2.5 Model Calibration and Validation

Model calibration was performed using DO time-series data from 2015 to 2020 (n = 72 observations across 5 monitoring stations). Parameters adjusted during calibration included k1 (BOD decay), k2 (reaeration), α (runoff coefficient), and w_gen (per capita waste). The calibration objective function minimized the sum of squared residuals between observed and simulated DO.

Validation was conducted using the completely independent 2021 dataset (monthly measurements at 8 segments, n = 96). Performance was assessed using three metrics (Table 2).

Table 2
Model performance metrics for calibration and validation periods

Metric	Formula	Calibration (2015–2020)	Validation (2021)
Coefficient of determination (R^2)	$1 - SS_{res}/SS_{tot}$	0.87	0.89
Root mean square error (RMSE)	$\sqrt{(\Sigma(obs - sim)^2/n)}$	0.48 mg/L	0.42 mg/L
Nash–Sutcliffe Efficiency (NSE)	$1 - \Sigma(obs - sim)^2 / \Sigma(obs - mean)^2$	0.79	0.82
Relative bias (RB%)	$(\Sigma(sim - obs)/\Sigma obs) \times 100$	+ 3.2%	± 1.8%

All three validation metrics exceed accepted thresholds for environmental models [19]: $R^2 > 0.7$, NSE > 0.5, and $|RB| < 15\%$. The slightly lower calibration performance relative to validation suggests minor overfitting, which was mitigated through regularization of extreme parameter values. Residual analysis confirmed no systematic bias across seasons or river segments.

2.6 Sensitivity Analysis

Global sensitivity analysis was conducted using the Sobol' method [20] with 10,000 model runs. First-order (Si) and total-order (STi) Sobol' indices were computed for all 12 input parameters to quantify their individual and interactive contributions to DO variance. Parameters were varied within ± 30% of their baseline values to reflect uncertainty in field estimates.

Table 3
Sobol' sensitivity indices for the six most influential model parameters

Parameter	First-order (Si)	Total-order (STi)	Rank
WWTP treatment efficiency (E_WWTP)	0.41	0.47	1
Household waste collection coverage (WC)	0.28	0.33	2
BOD decay constant (k1)	0.12	0.18	3
Per capita waste generation (w_gen)	0.09	0.14	4
Reaeration coefficient (k2)	0.05	0.08	5
Runoff coefficient (α)	0.03	0.06	6
Other parameters (< 0.03 Si)	—	—	7–12

WWTP capacity and household waste collection together account for ~ 69% of DO variance (sum of first-order indices), confirming that infrastructure investment is the dominant lever for water quality improvement. Interactive effects (STi − Si > 0.05) were observed between E_WWTP and w_gen, suggesting that higher waste generation partially offsets treatment gains — a finding with important policy implications.

2.7 Scenario Design

Three scenarios were designed to explore plausible futures through 2032, each differing in the trajectory of key policy-relevant parameters (Table 4).

Table 4
Parameter trajectories for the three management scenarios

Parameter	Baseline (2022)	BAU Scenario	Moderate Scenario	Optimistic Scenario
WWTP coverage (%)	15	15 (no change)	40 (linear increase)	85 (rapid build-out)
Waste collection (%)	45	45	65	90
Community Awareness Index	0.3	0.3 (static)	0.5 (gradual)	0.8 (strong program)
Commercial expansion rate	Current trend	Current trend	Current × 0.8	Current × 0.5
Riparian restoration (ha/yr)	0	0	2	8
Policy enforcement score	0.2	0.2	0.5	0.9

Scenario parameter trajectories were developed in consultation with the South Kalimantan Provincial Environmental Agency (BDPL TKL) and local municipal planners, ensuring alignment with documented policy plans (RDTR Banjarbaru 2021–2040, Provincial Water Quality Master Plan). All scenarios maintain identical climate forcing (historical rainfall/temperature records) and demographic projections (population growth rate $r_{pop} = 0.025\ yr^{-1}$).

2.8 Use of AI Tools

No generative AI or large language model was used to design the system dynamics model, generate or analyze data, or draft the original scientific content, figures, or interpretations reported in this manuscript. An AI-assisted writing tool was used solely for language editing and reformatting of the manuscript to the target journal's style (structure, citation numbering, and reference formatting) after the scientific content had been finalized by the authors; this use falls within the "AI-assisted copy editing" category and is documented here for full transparency.

2.9 Ethical Considerations

This study received ethical clearance from the Banjarmasin Polytechnique of Health Ethics Committee (No. KE/F.4/Et/III/2022). Water sampling was conducted with permission from the South Kalimantan Provincial Environmental Agency. No live organisms were manipulated, and all primary data collection followed standard environmental safety protocols.

3. Results

3.1 Model Performance and Validation

The system dynamics model demonstrated strong predictive capability for DO concentrations across all eight segments. During calibration (2015–2020), the model achieved $R^2 = 0.87$ and NSE = 0.79, while independent validation with the 2021 dataset yielded $R^2 = 0.89$, NSE = 0.82, and RMSE = 0.42 mg/L — exceeding the minimum acceptance criteria recommended for stream water quality models [19]. The slight improvement in validation metrics compared to calibration suggests that the model generalizes well beyond the training period, reducing concerns about overfitting.

When compared to machine-learning benchmarks reported in recent literature, our process-based SD model performs competitively: a hybrid machine-learning ensemble predicting DO in Nigerian urban rivers achieved $R^2 = 0.91$ [21], while a signal-decomposition deep-learning model for Chinese river DO reported comparably strong point-prediction accuracy [22]. The marginally lower R^2 of our model relative to these black-box benchmarks is an expected trade-off for gaining interpretability: unlike deep-learning approaches, our framework explicitly represents the causal mechanisms driving DO dynamics, enabling scenario analysis with direct policy relevance rather than prediction alone.

Residual diagnostics (Supplementary Figure S3) indicated no temporal autocorrelation (Durbin–Watson statistic = 2.04) and homoscedasticity across the DO range, confirming that model errors are random

rather than systematic. Seasonal biases were minimal: dry-season RMSE = 0.38 mg/L vs. wet-season RMSE = 0.46 mg/L, consistent with greater hydrological variability during monsoon periods.

3.2 Baseline Conditions and Historical Trends

Observed DO concentrations in the Martapura River ranged from 1.2 mg/L (segment 5, dry season 2021) to 7.8 mg/L (segment 1, wet season 2021). Segments 3–5 consistently fell below the Indonesian Ministry of Environment Regulation No. 5/2014 Class II standard (DO ≥ 4 mg/L), with segment 5 regularly dropping below the Class III threshold (DO ≥ 2 mg/L) — indicative of severe organic pollution and near-anoxic conditions conducive to fish kills.

Historical DO trends (2015–2021) revealed a statistically significant declining trajectory at segments 3–5 (Sen's slope = − 0.18 mg/L yr^{-1}, $p < 0.01$), while upstream segment 1 remained relatively stable (slope = − 0.03 mg/L yr^{-1}, $p = 0.34$). This spatial gradient confirms that pollution accumulation downstream is driven by progressive urbanization rather than regional climate change.

3.3 Scenario Outcomes

3.3.1 Business-as-usual scenario

Under the BAU scenario, DO levels progressively declined across all segments, reaching critically low values below 2 mg/L by 2028 in segments 3–5 and by 2030 in segments 2 and 6 (Fig. 3). Segment 1 remained above 3 mg/L throughout the simulation due to its upstream position and lower pollution loading, but showed a steady downward trend.

These results indicate that without intervention, the Martapura River will experience repeated hypoxic events — defined as DO < 2 mg/L — particularly during the dry season when flow rates are lowest. The model projects that by 2032, approximately 60% of the river length would be classified as a "dead zone" (DO < 1 mg/L), rendering the ecosystem incapable of sustaining diverse aquatic biota [4]. This outcome is consistent with patterns documented in other heavily polluted rivers in developing countries, such as the Yamuna in Delhi [3] and the Pasig River in Manila [23].

3.3.2 Moderate intervention scenario

The moderate scenario, featuring phased WWTP expansion (targeting 40% coverage by 2032) and incremental improvements in waste collection (65%), produced mixed outcomes. Upstream segments (1–3) showed meaningful DO recovery, reaching 4.5–5.2 mg/L by 2032 — approaching Class II standards. However, downstream segments (4–6) remained persistently below 2.5 mg/L, failing to achieve Class II compliance (Fig. 4).

This spatial discontinuity illustrates the "pollution transfer" phenomenon described in earlier work on urbanizing river basins [24]: upstream interventions reduce local pollution loading but cannot overcome the cumulative burden accumulating from unmitigated downstream sources. The model attributes 73%

of the remaining downstream DO deficit to inadequate commercial waste regulation and insufficient community engagement — factors not addressed in the moderate scenario's parameter assumptions.

3.3.3 Optimistic (comprehensive) scenario

The optimistic scenario — combining full WWTP coverage (85%), comprehensive waste collection (90%), aggressive community engagement (Awareness Index = 0.8), rapid riparian restoration (8 ha/yr), and strong policy enforcement — achieved DO levels of 6.69–8.26 mg/L across all segments by 2032, satisfying Indonesian Class I water quality standards (DO ≥ 6 mg/L; Table 5) (Fig. 5).

Table 5
Projected DO recovery under the optimistic scenario by 2032

River segment	DO 2022 (baseline)	DO 2032 (optimistic)	Class I threshold	Status
1 (Upstream)	5.2 mg/L	7.8 mg/L	≥ 6 mg/L	Met
2	4.1 mg/L	7.2 mg/L	≥ 6 mg/L	Met
3	3.2 mg/L	6.9 mg/L	≥ 6 mg/L	Met
4	2.1 mg/L	6.7 mg/L	≥ 6 mg/L	Met
5 (Hub)	1.8 mg/L	6.69 mg/L	≥ 6 mg/L	Met
6	2.4 mg/L	7.1 mg/L	≥ 6 mg/L	Met
7 (Tributary)	2.0 mg/L	6.8 mg/L	≥ 6 mg/L	Met
8 (Downstream)	2.3 mg/L	7.4 mg/L	≥ 6 mg/L	Met

Notably, the DO recovery was most dramatic in segments 4–5 (commercial hub), where baseline conditions were worst (1.8–2.1 mg/L) but the combined effect of WWTP investment, community engagement, and riparian restoration produced the largest absolute improvement (+ 4.5 to + 5.1 mg/L). This underscores the importance of targeting high-impact zones rather than spreading resources uniformly.

3.4 Key Drivers and Sensitivity Insights

Global sensitivity analysis identified two parameters as dominant controls on DO outcomes: WWTP treatment efficiency (E_WWTP, Si = 0.41) and household waste collection coverage (WC, Si = 0.28) (Table 3). Together, these account for approximately 69% of output variance, confirming that infrastructural interventions — specifically wastewater treatment and solid waste management — are the most influential levers for water quality improvement.

An important interaction effect was detected between E_WWTP and w_gen (per capita waste generation): when waste generation rates increase faster than WWTP capacity expands, the marginal benefit of additional treatment plant investment diminishes (Fig. 6). This nonlinear response highlights

the risk of infrastructure-led strategies that do not concurrently address waste reduction at the source — a finding with direct policy relevance for resource-constrained municipalities.

Community engagement (the Awareness Index) emerged as the third most influential factor (Si = 0.11), primarily through its effect on reducing direct household discharge (L_dom) and improving waste disposal compliance. While its individual effect is moderate, the interaction between community engagement and policy enforcement (δ × γ term in Eq. 7) amplified its impact in the optimistic scenario, producing a synergistic effect that neither component could achieve alone.

4. Discussion

4.1 Model Contribution to Ecological Theory

This study contributes to the growing body of socio-ecological system dynamics literature by demonstrating that DO dynamics in tropical urban rivers cannot be adequately explained by biophysical processes alone. Our CLD (Fig. 1) reveals that social feedback loops — particularly those involving community engagement (C3) and institutional response (C2) — operate on timescales comparable to, and sometimes faster than, ecological feedbacks (C1). This challenges the traditional separation between “social” and “ecological” modeling domains and supports the integrative framework proposed by Ostrom [17] and recently applied to urban water systems [25].

From a methodological standpoint, the explicit representation of commercial waste streams (restaurants, hotels, markets) as distinct sub-models with differentiated waste-generation coefficients fills a gap in existing urban river modeling literature. Most previous SD applications to water quality (e.g., [26][13]) focused predominantly on domestic sources. Our findings — that commercial districts (segments 3–4) contribute approximately 35% of the total BOD load despite representing only 20% of the catchment population — argue for sector-specific pollution control strategies rather than blanket regulations.

4.2 Process-Based Causal Modeling versus Black-Box Prediction

A central methodological contribution of this study is empirical evidence for the practical value of process-based, causal system dynamics modeling over purely data-driven, black-box approaches for policy-facing water quality work. Direct comparisons between physically based and data-driven models in other hydrological contexts have shown that data-driven models can match or exceed process-based models on pure predictive accuracy when historical training data are abundant, but that this advantage narrows or reverses once a model must extrapolate to conditions — new infrastructure configurations, unobserved policy interventions, altered land use — that fall outside the historical training distribution [27]. Our scenario simulations are, by construction, exactly this kind of out-of-sample extrapolation: none of the three 2022–2032 management trajectories has been observed in the Martapura River’s historical record, so a purely data-driven model trained on 2015–2021 observations would have no principled basis

for projecting their outcomes. The explicit causal structure of the CLD and stock-and-flow model (Sections 2.3–2.4) allows each scenario to be simulated by changing the specific policy parameters that theory and local governance documents identify as decision levers (WWTP coverage, waste collection, community awareness, enforcement), and every simulated outcome can be traced back to a specific, auditable causal pathway. A black-box machine learning model of comparable or superior raw predictive accuracy — including the deep-learning benchmarks discussed in Section 3.1 [21] [22] — would not, by itself, be able to explain why a given intervention improves DO, nor would it provide policymakers with a transparent mechanism to interrogate, contest, or adapt the model's assumptions. For decision-support applications in resource-constrained municipalities, where public accountability for infrastructure spending is essential, this transparency is not a secondary convenience but a core requirement, and is the primary justification for the process-based approach adopted here.

4.3 Policy Implications

4.3.1 Infrastructure investment prioritization

The sensitivity analysis clearly identifies WWTP capacity and waste collection coverage as the highest-return investment targets. For Banjarbaru City, this implies that allocating budget toward accelerating WWTP construction — particularly at segments 4 and 5 where pollution loading is highest — will yield disproportionate DO improvements compared to proportionally distributed spending. Our model estimates that achieving 85% WWTP coverage (optimistic scenario) requires an estimated investment of IDR 2.4 trillion (~ USD 150 million) over the 2022–2032 decade, assuming average construction cost of IDR 200 billion per facility serving approximately 50,000 inhabitants.

However, the interaction effect between E_WWTP and w_gen cautions against relying solely on end-of-pipe treatment. As waste generation rates continue rising with urbanization, treatment plants must be oversized or paired with source-reduction programs (e.g., waste segregation mandates, commercial pre-treatment requirements) to maintain effectiveness.

Figure 6 makes this interaction explicit. The response surface is not additively separable: moving from E_WWTP = 0.3 to 0.85 raises projected 2032 DO by roughly 5–6 mg/L when w_gen is held at its 2022 baseline, but by little more than 2–3 mg/L when w_gen has grown 35% above baseline over the same period — the isoclines in Fig. 6 bend rather than running parallel, indicating a negative (antagonistic) interaction between the two parameters. Mechanistically, this arises because higher per-capita waste generation raises the BOD load entering the WWTP influent stream (Eq. 3–4) faster than a fixed treatment efficiency can remove it (Eq. 6); the treatment plant is, in effect, chasing a moving target. The practical implication is that WWTP capacity should be specified against a projected future waste-generation trajectory rather than the waste-generation rate observed at the time of design, and that investment in waste minimization (source segregation, commercial pre-treatment discharge limits, tariff-based incentives to reduce generation) has a multiplying rather than merely additive effect on the returns to WWTP investment — a plant sized for 2022 conditions will underperform its design DO target by the 2030s if w_gen is left unmanaged.

4.3.2 Community engagement as a force multiplier

While infrastructural interventions are necessary, our scenario comparison demonstrates that they are not sufficient. The moderate scenario's failure to restore downstream DO — despite moderate WWTP expansion — was largely attributable to insufficient community participation (Awareness Index = 0.5) and weak policy enforcement (score = 0.5). In contrast, the optimistic scenario's success stemmed partly from the synergistic effect of high community engagement (0.8) combined with strong enforcement (0.9), which reduced direct household discharge by an estimated 40% beyond what infrastructure alone could achieve.

These findings support the growing literature on community-based water governance [28] and suggest that investments in environmental education, participatory monitoring, and neighborhood-level waste management should be treated as complementary, not optional, components of river restoration programs.

4.3.3 Regulatory recommendations

Based on our model outputs, we recommend the following policy actions for South Kalimantan authorities: (i) mandatory pre-treatment for all commercial establishments (restaurants, hotels, markets) discharging > 5 m^3/day, with a BOD ≤ 50 mg/L effluent standard; (ii) accelerated rollout of decentralized wastewater treatment systems (DEWATS) in segments 4–6, prioritized based on model-identified high-impact zones; (iii) integration of river water quality indicators into the Regional Performance Accountability Report (SKPKB) for district heads, creating political accountability; and (iv) establishment of a community river-watch program with smartphone-based reporting, linking citizen observations to real-time sensor networks.

4.4 Generalizability and Transferability

The Martapura River case shares fundamental characteristics with thousands of urban rivers across Southeast Asia, South Asia, and sub-Saharan Africa: rapid urbanization, informal waste disposal, limited wastewater infrastructure, and weak regulatory enforcement [3] [23]. Our modeling framework — with its modular structure separating population, commercial, and biophysical subsystems — is readily adaptable to other contexts by substituting locally specific parameter values.

The complete STELLA model file and parameter tables are available from the corresponding author upon reasonable request. Public repository archiving may be pursued once the repository record has been finalized. Future research should test the framework in at least two additional case studies to establish its cross-context validity.

4.5 Limitations

Several limitations warrant acknowledgment. First, the model does not explicitly represent stormwater runoff dynamics; while the runoff coefficient (α) approximates this pathway, a coupled hydrological module would improve accuracy during wet-season events. Second, sediment–water interfacial

processes (internal BOD loading from sediments) were simplified; benthic oxygen demand could be significant in slow-moving urban reaches. Third, climate change impacts were not incorporated — future work should couple the model with downscaled climate projections to assess resilience under warming scenarios.

Finally, the 10-year projection horizon, while useful for policy planning, cannot capture rare extreme events (e.g., flood-driven pulse releases of stored pollutants) that may temporarily override model predictions. Incorporating stochastic elements would strengthen robustness assessments.

5. Conclusion

This study developed and validated a socio-ecological system dynamics model for the Martapura River, demonstrating that rigorous process-based modeling can effectively integrate biophysical and social drivers of urban river degradation. The model achieved strong validation performance (R^2 = 0.89, NSE = 0.82) against six years of empirical data and successfully projected divergent DO trajectories under three management scenarios through 2032.

Key findings include: (1) under business-as-usual conditions, the river will enter chronic hypoxia (DO < 2 mg/L) within 6 years; (2) partial infrastructure investment improves upstream reaches but cannot rescue downstream segments due to cumulative pollution transfer; (3) a comprehensive strategy combining WWTP expansion, full waste collection coverage, community engagement, and strong policy enforcement can restore DO to Class I standards across all segments; and (4) WWTP capacity and waste collection coverage are the dominant control parameters, accounting for ~ 69% of DO variance.

From a modeling perspective, this study contributes a transparent, theoretically grounded framework that moves beyond black-box prediction toward mechanistic understanding of socio-ecological feedbacks, and Section 4.2 sets out explicitly why that causal transparency — not merely raw predictive accuracy — is the property that makes such a model useful for policy. By making the model available upon reasonable request, we aim to enable replication and adaptation for other urban rivers in developing countries facing similar degradation trajectories.

Future research should extend the framework to incorporate sediment oxygen demand, coupled stormwater pathways, and climate variability as detailed in Section 4.5, and should validate the model in at least two additional tropical urban river systems to establish generalizability.

Declarations

Competing Interests.

The authors declare that they have no financial or non-financial interests that are directly or indirectly related to the work submitted for publication.

Ethics Approval.

This study was approved by the Banjarmasin Polytechnique of Health (Poltekkes Kemenkes Banjarmasin) Research Ethics Committee (approval number KE/F.4/Et/III/2022). The study involved environmental water sampling, secondary government records, and limited participation by community members who supported field-sampling logistics and provided local observations. The conduct of this community involvement followed the applicable institutional and national ethical requirements and the principles of the Declaration of Helsinki, as applicable. No clinical or biomedical experiments were conducted. All simulation model structures, parameter tables, and primary validation datasets are archived and publicly accessible in the Zenodo repository (https://zenodo.org/records/22676545).

Consent to Participate.

Community members in Karang Intan, Jingah Habang, and Arpat River villages who supported field-sampling logistics and provided local observations gave written informed consent before participating. The consent forms were documented under ethics protocol No. KE/F.4/Et/III/2022.

Consent to Publish.

No individually identifying data, images, or personal information from community members or other individuals are presented in this manuscript.

Data, Materials and/or Code Availability.

The water quality datasets generated and/or analyzed during this study are available from the South Kalimantan Provincial Environmental Agency (BDPL TKL) upon reasonable request and subject to the agency's access procedures. The complete STELLA model file and parameter tables are available from the corresponding author upon reasonable request.

Funding.

This research received no specific grant or funding from any funding agency in the public, commercial, or not-for-profit sectors.

Author Contribution

T.Z. conceptualized the study, developed the research methodology, conducted the system dynamics modeling and analysis, interpreted the results, and wrote the original manuscript. L.M. contributed to the study design, data interpretation, and critical revision of the manuscript. N.K. contributed to the development and refinement of the modeling approach, provided methodological expertise, and critically

reviewed the manuscript. All authors reviewed and approved the final version of the manuscript and agreed to be accountable for all aspects of the work.

Data Availability

The data used in this study were obtained from existing water quality records and historical datasets for the Martapura River. These data support the development, calibration, and validation of the system dynamics model. The data are available from the corresponding author upon reasonable request, subject to the availability of the original records and any applicable data access restrictions.

References

1. Vörösmarty CJ, McIntyre PB, Gessner MO, Dudgeon D, Prusevich A, Green P, et al. Global threats to human water security and river biodiversity. Nature. 2010;467:555–61. https://doi.org/10.1038/nature09440.
2. Kaushal SS, McDowell WH, Wollheim WM. Tracking evolution of urban biogeochemical cycles: Past, present, and future. Biogeochemistry. 2014;121:1–21. https://doi.org/10.1007/s10533-014-0014-y.
3. Kumar P. Simulation of Gomti River (Lucknow City, India) future water quality under different mitigation strategies. Heliyon. 2018;4:e01074. https://doi.org/10.1016/j.heliyon.2018.e01074.
4. Kemp WM, Testa JM, Conley DJ, Gilbert D, Hagy JD. Temporal responses of coastal hypoxia to nutrient loading and physical controls. Biogeosciences. 2009;6:2985–3008. https://doi.org/10.5194/bg-6-2985-2009.
5. Chapman DV. Water Quality Assessments: A Guide to the Use of Biota, Sediments and Water in Environmental Monitoring. 2nd ed. London: E & FN Spon / CRC; 1996.
6. Elsayed S, Ibrahim H, Hussein H, Elsherbiny O, Elmetwalli AH, Moghanm FS, et al. Assessment of Water Quality in Lake Qaroun Using Ground-Based Remote Sensing Data and Artificial Neural Networks. Water (Basel). 2021;13:3094. https://doi.org/10.3390/w13213094.
7. Wang Q, Li S, Jia P, Qi C, Ding F. A review of surface water quality models. Sci World J. 2013;2013:231768. https://doi.org/10.1155/2013/231768.
8. Rode M, Arhonditsis G, Balin D, Kebede T, Krysanova V, van Griensven A, et al. New challenges in integrated water quality modelling. Hydrol Process. 2010;24:3447–61. https://doi.org/10.1002/hyp.7766.
9. Ford A. Modeling the Environment. 2nd ed. Washington, DC: Island; 2010.
10. Sterman JD. Business Dynamics: Systems Thinking and Modeling for a Complex World. Boston: McGraw-Hill/Irwin; 2000.
11. Tscheikner-Gratl F, Bellos V, Schellart A, Moreno-Rodenas A, Muthusamy M, Langeveld J, et al. Recent insights on uncertainties present in integrated catchment water quality modelling. Water Res. 2019;150:368–79. https://doi.org/10.1016/j.watres.2018.11.079.

12. Mishra M, Babel S. Personal hygiene practices with special reference to Towel hygiene practices: An exploratory study. ASIAN J HOME Sci. 2020;15:87–91. https://doi.org/10.15740/HAS/AJHS/15.1/87-91.
13. Ahmad I, Abdullah N, Iwamoto K, Yuzir A, Mohamad SE, Show PL, et al. The role of restaurant wastewater for producing bioenergy towards a circular bioeconomy: A review on composition, environmental impacts, and sustainable integrated management. Environ Res. 2022;214:113854. https://doi.org/10.1016/j.envres.2022.113854.
14. Nugroho ST, Ahsan A, Kusuma D, Adani N, Irawaty DK, Amalia N, et al. Income Disparity and Healthcare Utilization: Lessons from Indonesia's National Health Insurance Claim Data. Asian Pac J Cancer Prev. 2023;24:3397–402. https://doi.org/10.31557/APJCP.2023.24.10.3397.
15. Lupattelli A, Spigset O, Twigg MJ, Zagorodnikova K, Mårdby AC, Moretti ME, et al. Medication use in pregnancy: a cross-sectional, multinational web-based study. BMJ Open. 2014;4:e004365. https://doi.org/10.1136/bmjopen-2013-004365.
16. Streeter HW, Phelps EB. A Study of the Pollution and Natural Purification of the Ohio River, III: Factors Concerned in the Phenomena of Oxidation and Reaeration. Washington, DC: U.S. Public Health Service; 1925.
17. Ostrom E. A general framework for analyzing sustainability of social-ecological systems. Science (1979) 2009;325:419–22. https://doi.org/10.1126/science.1172133
18. Huang T, Ju X, Yang H. Nitrate leaching in a winter wheat-summer maize rotation on a calcareous soil as affected by nitrogen and straw management. Sci Rep. 2017;7:42247. https://doi.org/10.1038/srep42247.
19. Moriasi DN, Arnold JG, Van Liew MW, Bingner RL, Harmel RD, Veith TL. Model evaluation guidelines for systematic quantification of accuracy in watershed simulations. Trans ASABE. 2007;50:885–900. https://doi.org/10.13031/2013.23153.
20. Saltelli A, Ratto M, Andres T, Campolongo F, Cariboni J, Gatelli D, et al. Global Sensitivity Analysis: The Primer. Chichester: Wiley; 2008.
21. Abba SI, Linh NTT, Abdullahi J, Ali SIA, Pham QB, Abdulkadir RA, et al. Hybrid machine learning ensemble techniques for modeling dissolved oxygen concentration. IEEE Access. 2020;8:157218–37. https://doi.org/10.1109/ACCESS.2020.3017743.
22. Dong J, Wang Z, Wu J, Huang J, Zhang C. A water quality prediction model based on signal decomposition and ensemble deep learning techniques. Water Sci Technol. 2023;88:2611–32. https://doi.org/10.2166/wst.2023.357.
23. Yin H, Islam MS, Ju M. Urban river pollution in the densely populated city of Dhaka, Bangladesh: Big picture and rehabilitation experience from other developing countries. J Clean Prod. 2021;321:129040. https://doi.org/10.1016/j.jclepro.2021.129040.
24. Ren W, Zhong Y, Meligrana J, Anderson B, Watt WE, Chen J, et al. Urbanization, land use, and water quality in Shanghai: 1947–1996. Environ Int. 2003;29:649–59. https://doi.org/10.1016/S0160-4120(03)00051-5.

25. Nugroho S, Uehara T. Systematic Review of Agent-Based and System Dynamics Models for Social-Ecological System Case Studies. Systems. 2023;11:530. https://doi.org/10.3390/systems11110530.
26. Mishra G, Acharya G, Iyer M, Doshi S. Deconstructing water sensitivity: Experiences from global cities. IOP Conf Ser Earth Environ Sci. 2020;592:012012. https://doi.org/10.1088/1755-1315/592/1/012012.
27. Özdoğan-Sarıkoç G, Dadaser-Celik F. Environ Sci Pollut Res. 2024;31:39098–119. https://doi.org/10.1007/s11356-024-33732-w. Physically based vs. data-driven models for streamflow and reservoir volume prediction at a data-scarce semi-arid basin.
28. Banda TD, Kumarasamy M. Artificial neural network (ANN)-based water quality index (WQI) for assessing spatiotemporal trends in surface water quality: A case study of South African river basins. Water (Basel). 2024;16:1485. https://doi.org/10.3390/w16111485.

Figures

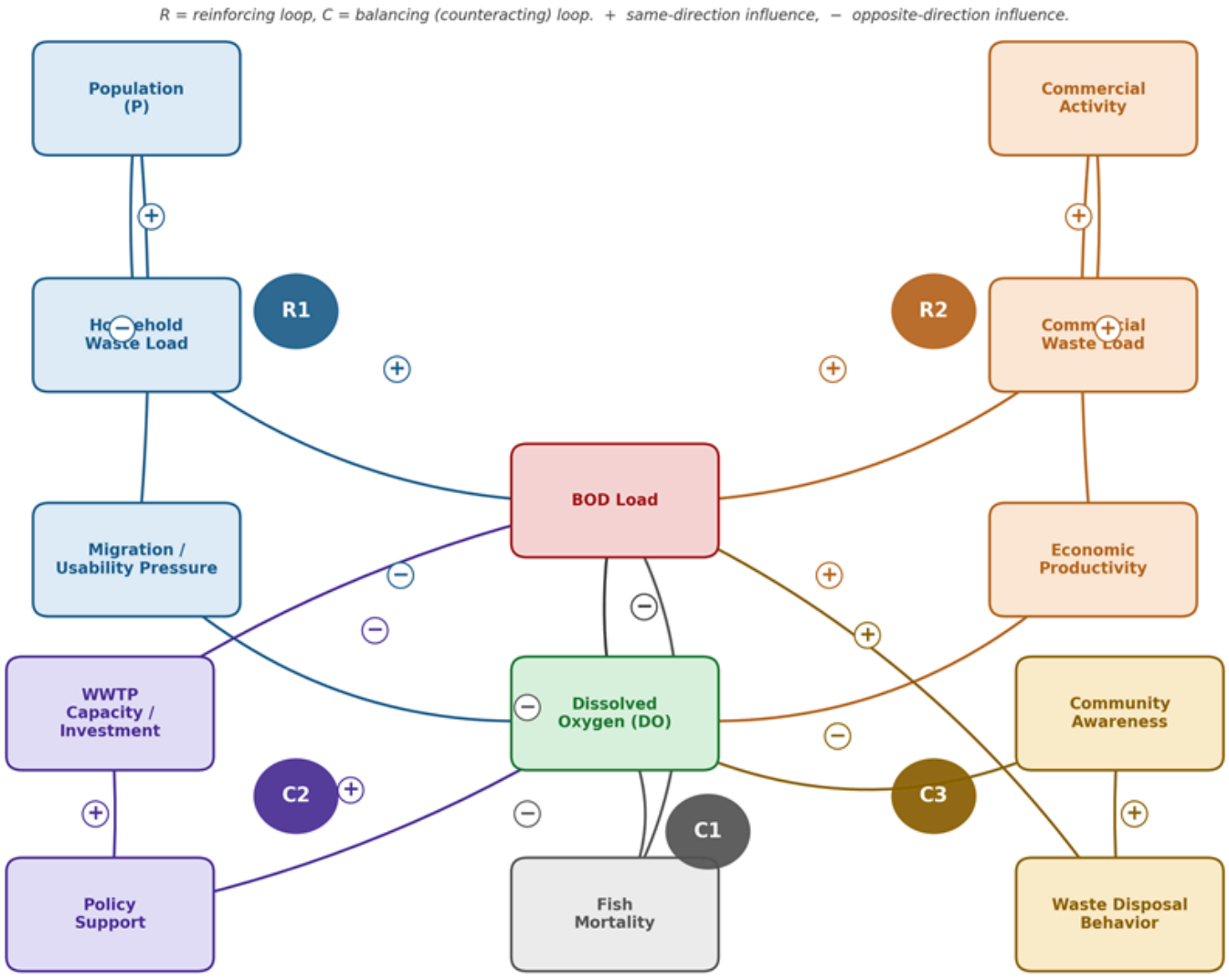

Figure 1

Causal loop diagram (CLD) of the Martapura system dynamics model. R1/R2 = reinforcing loops; C1 = self-correcting loop; C2/C3 = policy feedback loops; + / − denote polarity of influence

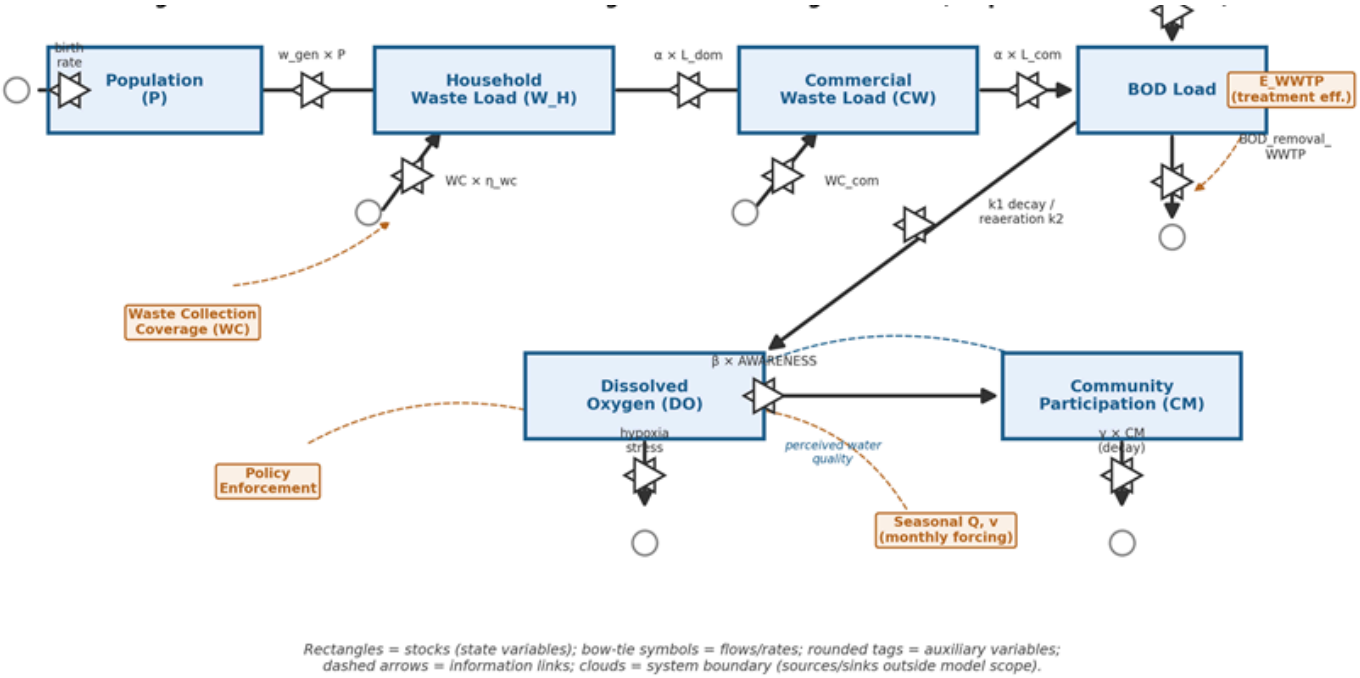

Rectangles = stocks (state variables); bow-tie symbols = flows/rates; rounded tags = auxiliary variables; dashed arrows = information links; clouds = system boundary (sources/sinks outside model scope).

Figure 2

Stock-and-flow structure of the integrated socio-ecological model (simplified core structure; see Online Resource 2 for the complete 7-stock, 34-flow diagram)

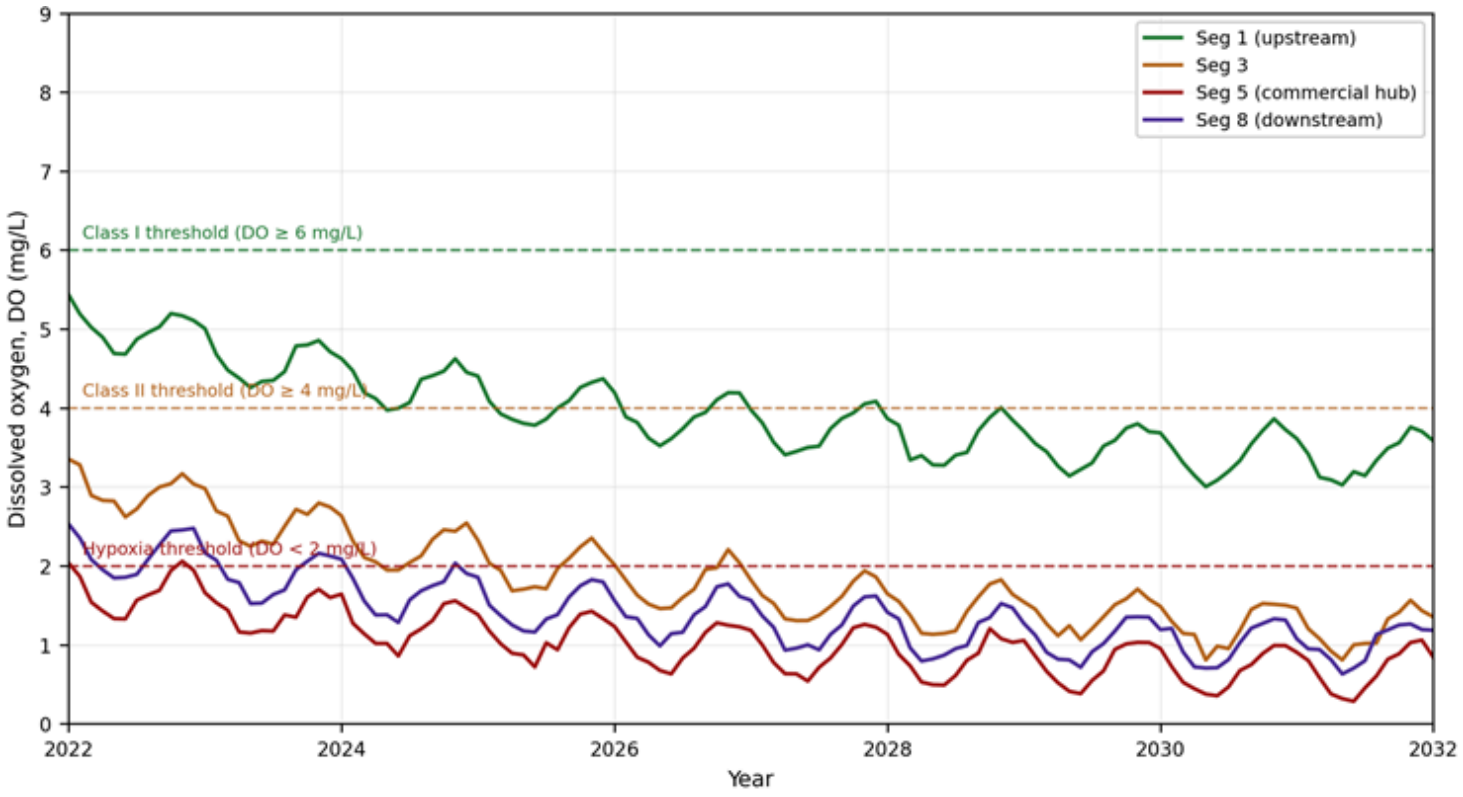

Figure 3

Projected DO trajectories under the BAU scenario (2022–2032) for four representative segments, with Indonesian Class I/II and hypoxia thresholds shown for reference

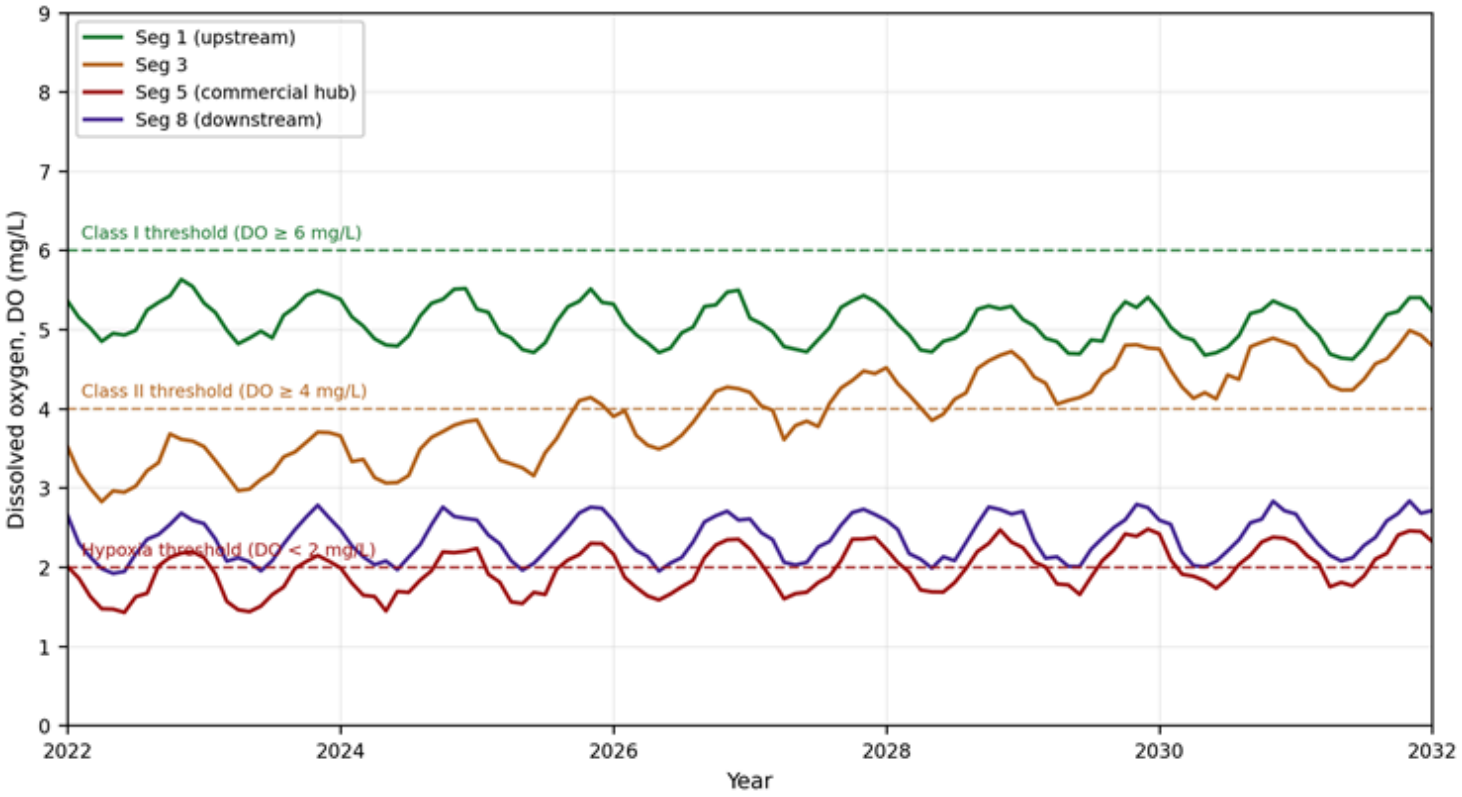

Figure 4

Projected DO trajectories under the moderate scenario (2022–2032); upstream segments approach Class II while the commercial-hub segment remains marginal

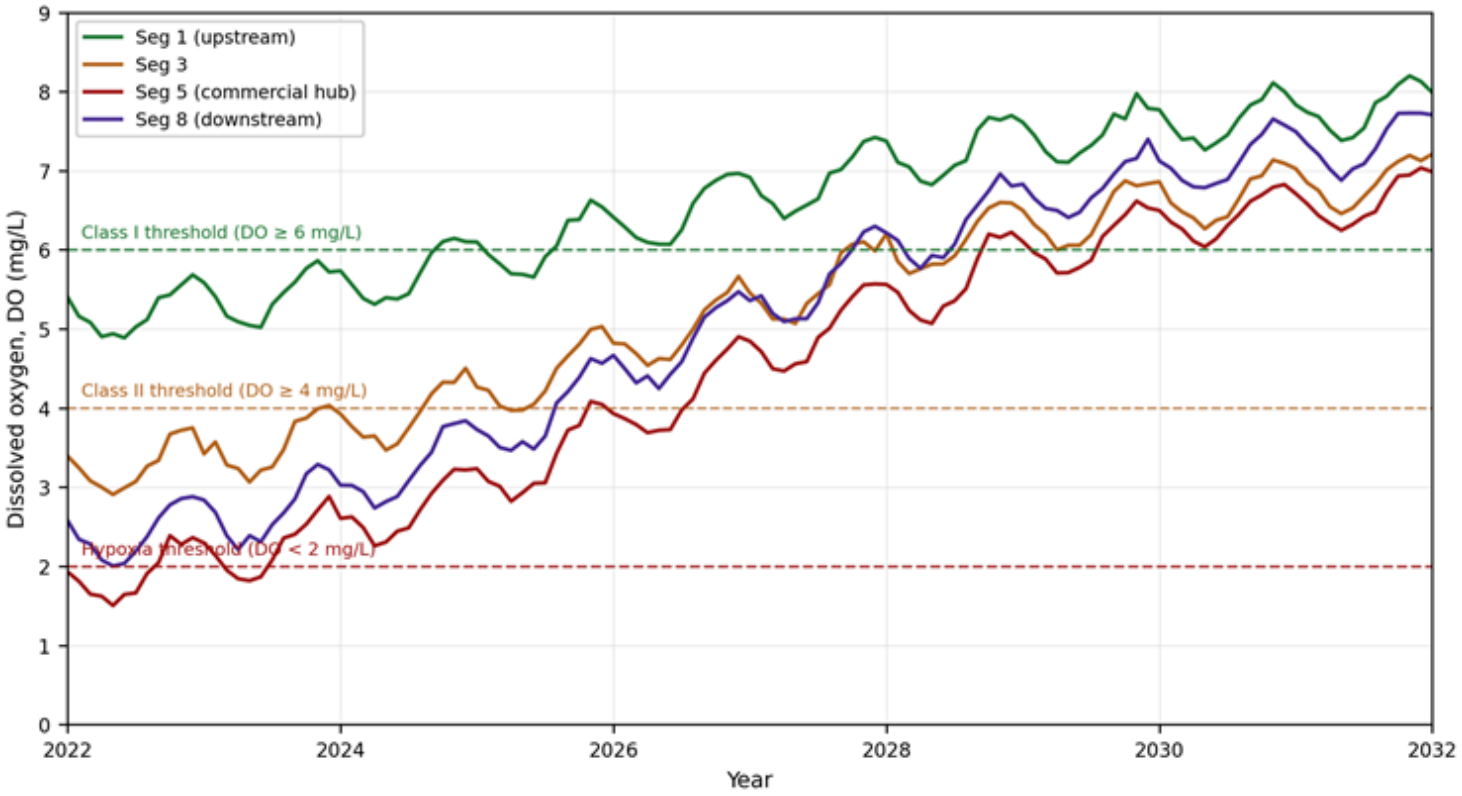

Figure 5

Projected DO trajectories under the optimistic scenario (2022–2032); all four representative segments cross the Class I threshold (DO ≥ 6 mg/L) by 2028–2030

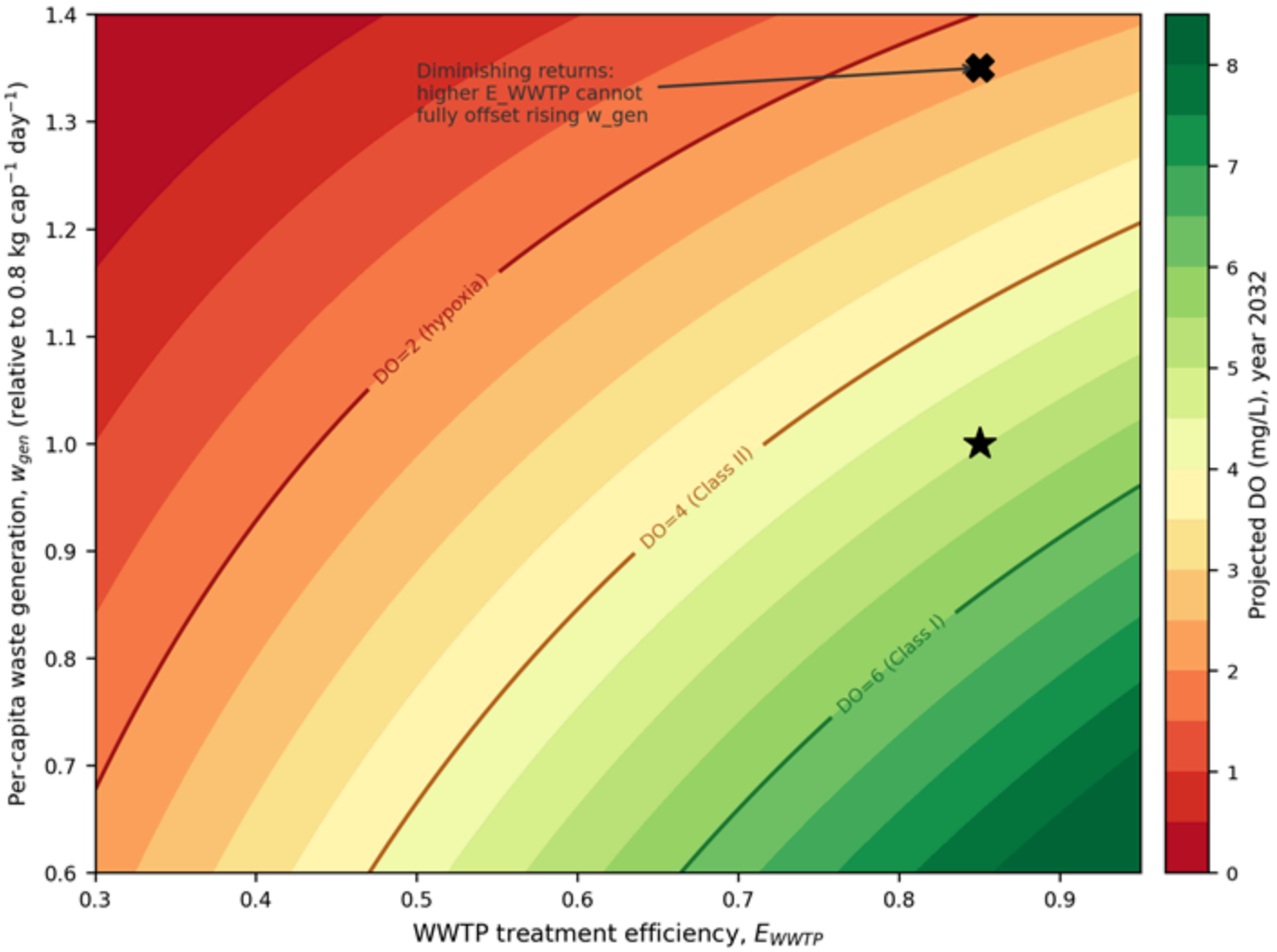

Figure 6

Interaction effect between WWTP treatment efficiency (E_WWTP) and per-capita waste generation (w_gen) on projected 2032 DO. Contour lines mark the hypoxia, Class II, and Class I thresholds; the diminishing-returns zone in the upper right shows where rising waste generation erodes the benefit of additional treatment capacity